[3]Srinivasan, R., and Mongia, H. C., "Numerical Computation of Swirling Recirculating Flows," NASA CR 165197, Sept. 1980.

[4]Hogg, S., and Leschziner, M. A., "Computation of Highly Swirling Confined Flow with a Reynolds Stress Turbulence Model," *AIAA Journal*, Vol. 27, No. 1, 1989, pp. 57–63.

[5]Jones, W. P., and Pascau, A., "Calculation of Confined Swirling Flows with a Second Moment Closure," *Journal of Fluids Engineering*, Vol. 111, Sept. 1989, pp. 248–255.

[6]Gibson, M. M., and Launder, B. E., "Ground Effects on Pressure Fluctuations in the Atmospheric Boundary Layer," *Journal of Fluid Mechanics*, Vol. 86, April 1978, pp. 491–511.

[7]Yakhot, V., Orszag, S. A., Thangam, S., Gatski, T. B., and Speziale, C. G., "Development of Turbulence Models for Shear Flows by a Double Expansion Technique," *Physics of Fluids A*, Vol. 4, No. 7, 1992, pp. 1510–1520.

[8]Launder, B. E., and Spalding, D. B., "The Numerical Computation of Turbulent Flows," *Computer Methods in Applied Mechanics and Engineering*, Vol. 3, May 1974, pp. 269–289.

[9]Nejad, A. S., Favaloro, S. C., Vanka, S. P., Samimy, M., and Langenfeld. C., "Application of Laser Velocimetry for Characteristics of Confined Swirling Flow," *Journal of Engineering for Gas Turbines and Power*, Vol. 111, No. 1, 1989, pp. 36–45.

[10]van Doormal, J. P., and Raithby, G. D., "Enhancement of the SIMPLE Method for Predicting Incompressible Fluid Flows," *Numerical Heat Transfer*, Vol. 7, No. 2, 1984, pp. 147–163.

[11]Lai, Y. G., So, R. M. C., and Przekwas, A. J., "Turbulent Transonic Flow Simulation Using a Pressure-Based Method," *International Journal of Engineering Science*, Vol. 33, No. 4, 1995, pp. 469–483.

[12]Lai, Y. G., "Computational Method of Second-Moment Turbulence Closures in Complex Geometries," *AIAA Journal*, Vol. 33, No. 8, 1995, pp. 1426–1432.

[13]Favaloro, S., Nejad, A., Ahmed, S., Miller, T., and Vanka, S., "An Experimental and Computational Investigation of Isothermal Swirling Flow in an Axisymmetric Dump Combustor," AIAA Paper 89-0620, Jan. 1989.

[14]Speziale, C. G., and Thangam, S., "Analysis of an RNG Based Turbulence Model for Separated Flows," NASA CR 189600, Jan. 1992.

Ionizational Nonequilibrium Induced by Neutral Chemistry in Air Plasmas

Christophe O. Laux,* Richard J. Gessman,† and Charles H. Kruger‡

Stanford University, Stanford, California 94305-3032

Introduction

IONIZATIONAL nonequilibrium in plasmas can greatly affect the reactivity, transport properties (thermal and electrical conductivity), and radiative phenomena because of collisional coupling between the populations of bound and free electrons. Normally, departures from equilibrium in the population of free electrons are attributed to either (or both) differences between electron and gas kinetic temperatures or finite ionization/electron recombination rates. In contrast, the computational study reported here for a recombining air plasma suggests that under appropriate circumstances ionizational nonequilibrium may be caused instead by finite dissociation/recombination rates for neutral species. Thus we find the unexpected result that nonequilibrium populations of neutral species can cause ionizational nonequilibrium in molecular plasmas. The consequences of this effect on the radiative power of NO in air plasmas are examined.

Model

This study considers ionizational nonequilibrium in a recombining air plasma assumed to be thermal (equal electron and heavy particle temperatures). Although the phenomena described herein are by no means limited to thermal plasmas, they can be described more clearly with a single temperature plasma. The Chemkin solver[1] was used for one-dimensional kinetics modeling with specified initial concentrations and with imposed temperature variations. Three air reaction mechanisms [Dunn and Kang,[2] Gupta et al. (GYTL),[3] and Park[4,5]] were considered. Reverse reaction rates were obtained by detailed balance using the equilibrium thermodynamic properties computed by Liu and Vinokur.[6] The air plasma was assumed to be initially in chemical equilibrium at 7500 K and 1 atm. A linear temperature drop from 7500 to 4500 K within 0.6 ms was then imposed on the plasma, and the concentration evolution of the major neutral and charged species was computed with Chemkin. At each time, concentrations were normalized to their chemical equilibrium values at the corresponding temperature. The resulting normalized concentrations, or nonequilibrium factors, are shown in Fig. 1. Observations derived from these results are discussed in the next section.

To check the thermal plasma assumption, we have calculated the differences between the electron kinetic temperature T_e, the gas kinetic temperature T_h, and the vibrational temperature T_v and found that they are negligible for the conditions of this Note. For molecular plasmas with no applied external field, the electron energy equation[7] is

$$3n_e \sum_{\text{species } s} \frac{m_e}{m_s} \bar{\nu}_{es} \delta_s k (T_e - T_h) = \sum_{\text{ion } i} \varepsilon_i \frac{\partial n_i}{\partial t}\bigg|_{\text{3 body-recombination}} \tag{1}$$

where n_e, m_e, and m_s represent the electron number density, the electron mass, and the mass of heavy species s, respectively; δ_s is the so-called nonelastic energy loss factor, used as a multiplier to the rate of energy transferred by elastic collisions to model the effect of nonelastic collisions; and the term on the right-hand side represents the net rate of energy transferred to the electrons by three-body ion

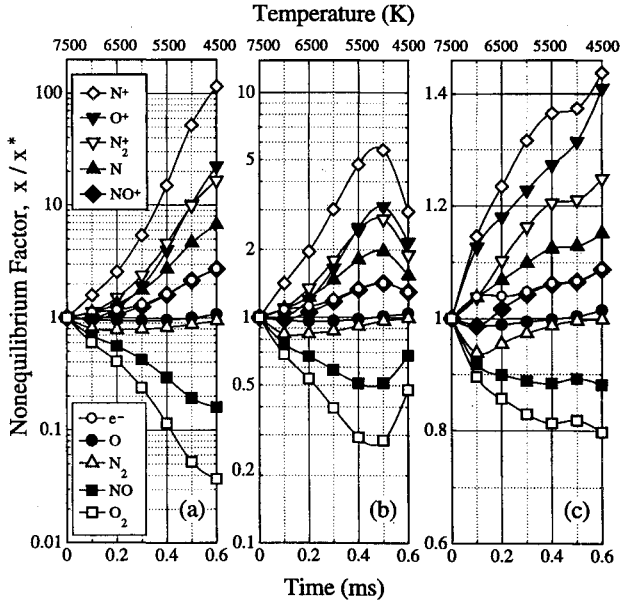

Fig. 1 Nonequilibrium factors predicted with the reaction mechanisms of a) Dunn and Kang, b) GYTL, and c) Park. The validity of Eqs. (2), (4), and (5) for $t > 0.3$ ms can be verified from these figures. For instance, that the electron overpopulation factor varies as the square root of the N overpopulation factor [Eq. (4)] can be seen most easily in the logarithmic plots (a and b), where the electron overpopulation curve lies half the distance from the equilibrium line ($x/x^* = 1$) to the N overpopulation curve.

Received May 25, 1994; revision received Feb. 2, 1996; accepted for publication April 22, 1996.

*Research Associate, High Temperature Gasdynamics Laboratory. Member AIAA.

†Graduate Student, High Temperature Gasdynamics Laboratory. Student Member AIAA.

‡Professor, Vice-Provost, and Dean of Research and Graduate Policy, High Temperature Gasdynamics Laboratory. Member AIAA.

Table 1 State of Dunn and Kang mechanism at $t = 0.6$ ms, with reactions listed in order of decreasing efficiency

Reaction	Forward rate F, mole-cm^{-3}-s^{-1}	Reverse rate R, mole-cm^{-3}-s^{-1}	$\log_{10}\lvert F-R\rvert$	$(R-F)/(F+R)$
1. $O + N_2 \Leftrightarrow N + NO$	$2.261E{-}02$	$2.355E{-}02$	-3.03	0.020
2. $O + NO \Leftrightarrow N + O_2$	$2.003E{-}03$	$2.881E{-}03$	-3.06	0.180
3. $O_2 + O \Leftrightarrow 3O$	$2.534E{-}05$	$7.987E{-}04$	-3.11	0.939
4. $O_2 + N_2 \Leftrightarrow 2O + N_2$	$3.713E{-}06$	$1.170E{-}04$	-3.95	0.939
5. $NO + O \Leftrightarrow N + 2O$	$1.481E{-}06$	$6.712E{-}05$	-4.18	0.957
6. $NO + N_2 \Leftrightarrow N + O + N_2$	$1.356E{-}06$	$6.147E{-}05$	-4.22	0.957
7. $N + N_2 \Leftrightarrow 3N$	$3.650E{-}07$	$1.723E{-}05$	-4.77	0.959
8. $2N_2 \Leftrightarrow 2N + N_2$	$2.396E{-}07$	$1.131E{-}05$	-4.96	0.959
9. $NO + N \Leftrightarrow O + 2N$	$2.140E{-}07$	$9.700E{-}06$	-5.02	0.957
10. $O_2 + N \Leftrightarrow 2O + N$	$1.465E{-}07$	$4.617E{-}06$	-5.35	0.939
11. $N_2 + O \Leftrightarrow 2N + O$	$5.287E{-}08$	$2.496E{-}06$	-5.61	0.959
12. $O + N \Leftrightarrow NO^+ + e$	$4.178E{-}05$	$4.305E{-}05$	-5.90	0.015
13. $2NO \Leftrightarrow N + O + NO$	$2.001E{-}08$	$9.071E{-}07$	-6.05	0.957
14. $O_2 + NO \Leftrightarrow 2O + NO$	$1.370E{-}08$	$4.318E{-}07$	-6.38	0.939
15. $2O_2 \Leftrightarrow 2O + O_2$	$7.788E{-}09$	$2.455E{-}07$	-6.62	0.939
16. $N_2 + NO \Leftrightarrow 2N + NO$	$7.146E{-}10$	$3.373E{-}08$	-7.48	0.959
17. $NO + O_2 \Leftrightarrow N + O + O_2$	$6.320E{-}10$	$2.865E{-}08$	-7.55	0.957
18. $O + NO^+ \Leftrightarrow NO + O^+$	$2.715E{-}08$	$3.260E{-}08$	-8.26	0.091
19. $NO + N_2 \Leftrightarrow NO^+ + e + N_2$	$8.876E{-}11$	$4.145E{-}09$	-8.39	0.958
20. $O + e \Leftrightarrow O^+ + 2e$	$4.434E{-}11$	$2.487E{-}09$	-8.61	0.965
21. $N_2 + O_2 \Leftrightarrow 2N + O_2$	$4.513E{-}11$	$2.130E{-}09$	-8.68	0.959
22. $N + NO^+ \Leftrightarrow NO + N^+$	$6.979E{-}08$	$7.092E{-}08$	-8.95	0.008
23. $2N \Leftrightarrow N_2^+ + e$	$6.861E{-}08$	$6.938E{-}08$	-9.12	0.006
24. $N_2 + O^+ \Leftrightarrow O + N_2^+$	$5.093E{-}09$	$4.334E{-}09$	-9.12	-0.080
25. $N + N_2^+ \Leftrightarrow N_2 + N^+$	$1.125E{-}07$	$1.119E{-}07$	-9.19	-0.003
26. $O + NO^+ \Leftrightarrow O_2 + N^+$	$5.899E{-}10$	$8.621E{-}10$	-9.57	0.187
27. $N + e \Leftrightarrow N^+ + 2e$	$2.455E{-}13$	$1.165E{-}11$	-10.94	0.959
28. $NO + O_2 \Leftrightarrow NO^+ + e + O_2$	$1.655E{-}13$	$7.728E{-}12$	-11.12	0.958
29. $O_2 + N_2 \Leftrightarrow NO + NO^+ + e$	$8.280E{-}16$	$2.800E{-}14$	-13.57	0.943

recombination reactions. [Note that the (exothermic) dissociative recombination reaction $NO^+ + e \Leftrightarrow N + O$, which is the principal electron recombination channel here, increases not the electron temperature but instead the thermal energy of the gas.] Using the nonelastic energy loss factors of Ref. 8, Eq. (1) predicts that, for all three reaction mechanisms, the differences between gas and electron kinetic temperatures are no more than 25 K throughout the reaction zone. That the translational and vibrational modes of heavy particles are equilibrated can be shown in turn by comparing the characteristic flow time, 600 μs here, to the slowest vibrational relaxation time of plasma species, 20 μs here [because for the present conditions the slowest vibrational relaxation rate parameter $p_c\tau$ is 2×10^{-5} atm-s (Ref. 4, p. 59)]. As the flow time is more than 30 times greater than the vibrational time, it is clear that the translational and vibrational modes are equilibrated.

Results

Mechanism of Dunn and Kang

With this mechanism, Chemkin predicts (see Fig. 1) that O and N_2 remain essentially in equilibrium, whereas N, O_2, and NO populations depart from equilibrium by one to two orders of magnitude. (By equilibrium we mean that the concentrations at a given temperature and pressure are nearly equal to their global equilibrium values, not that O and N_2 are in equilibrium with O_2 and N, respectively.) Charged species populations also deviate from equilibrium. In particular, the electron overpopulation factor reaches approximately three at time $t = 0.6$ ms.

To understand the process leading to ionizational nonequilibrium, it is instructive to examine the reaction rates. Listed in Table 1 for each reaction are the forward and reverse rates at $t = 0.6$ ms ($T = 4500$ K), as well as their differences. These differences represent the net rate of production/destruction of species by a given reaction and can be used to rank the reactions. Accordingly, the reactions in Table 1 are listed by order of decreasing efficiency. The last column of the table contains for each reaction the ratio between the difference and the sum of the rates. When this ratio is close to zero, the reaction is equilibrated; a value close to unity indicates nonequilibrium. The following analysis is based on the inspection of the rates at 0.6 ms but is equally valid at any prior time $t \geq 0.3$ ms.

First, we consider the chemistry of neutral species. Reactions 1–3 in Table 1 are the most efficient reactions, by at least one order of magnitude. Since their net rates are approximately equal, these reactions overall promote N recombination ($2N \rightarrow N_2$) while maintaining O, O_2, and NO close to quasi-steady state (QSS). [Interestingly, the Zel'dovich reactions (reactions 1 and 2 in Table 1) produce O and N_2 while maintaining NO in QSS. To readers more familiar with combustion environments where the endothermic $O + N_2 \rightarrow N + NO$ and exothermic $N + O_2 \rightarrow O + NO$ reactions combine to produce NO while N atoms remain in QSS, this may appear surprising. Here, the atypical behavior arises because the concentration of N atoms is much higher than in flames and thus causes reaction 1 to proceed from right to left, the opposite from combustion.] Therefore, for the conditions considered, only small concentration changes occur for O, O_2, and NO. Between 7500 and 4500 K, O atoms represent between 99 and 90% of the oxygen-containing species and remain close to chemical equilibrium. In contrast, the populations of O_2 and NO are below their chemical equilibrium values because the mole fraction increases required to reach equilibrium at 4500 K from initially equilibrium at 7500 K, equal to 439 and 19, respectively, are too large to be compatible with approximate QSS. Finally, nitrogen recombination reactions are fast enough to maintain N_2 in equilibrium (only a factor 5 increase in N_2 mole fraction is necessary), but not to keep N itself in chemical equilibrium (a factor 91 mole fraction decrease would be required). Quantitatively, since N_2 and O are close to equilibrium and since reactions 1 and 2 are essentially equilibrated, we have

$$[NO]/[NO]^* \cong ([N]/[N]^*)^{-1}, \qquad [O_2]/[O_2]^* \cong ([N]/[N]^*)^{-2} \tag{2}$$

where the asterisks denote equilibrium concentrations. Thus the chemistry of neutral species is controlled by N atom recombination reactions.

Second, Table 1 shows that reaction 12 ($NO^+ + e \Leftrightarrow N + O$) is the main channel for electron recombination since its net rate is much greater than the rates of the other electron recombination reactions

(19, 20, 23, and 27–29). Also, it is equilibrated, and therefore we have

$$\frac{[NO^+][e^-]}{[N][O]} \cong \left(\frac{[NO^+][e^-]}{[N][O]}\right)^* \tag{3}$$

Noting that NO^+ is the major ion and (see Fig. 1) that $[O] \cong [O]^*$, it follows that

$$[e^-]/[e^-]^* \cong \sqrt{[N]/[N]^*} \cong [NO^+]/[NO^+]^* \tag{4}$$

Furthermore, since all charge-exchange (18, 22, 24, 25) and charge-transfer (26) reactions are close to equilibrium, the following relations are also verified:

$$[N^+]/[N^+]^* \cong ([N]/[N]^*)^{\frac{5}{2}}, \qquad [O^+]/[O^+]^* \cong ([N]/[N]^*)^{\frac{3}{2}}$$
$$\left[N_2^+\right]/\left[N_2^+\right]^* \cong ([N]/[N]^*)^{\frac{3}{2}} \tag{5}$$

Excess free-electron (and ion) densities are caused therefore by elevated N atom concentrations, which themselves result from finite N recombination rates. Thus we have the result, suggested earlier,[9] that ionizational nonequilibrium is caused by the slow recombination of neutrals.

Mechanism of GYTL

The model of GYTL[3] differs from the Dunn and Kang[2] model only in the rates for dissociative electron recombination, $NO^+ + e \Leftrightarrow N + O$, and for three-body thermal association, $N + O + M \Leftrightarrow NO + M$. The most significant difference is for the latter reaction as the catalytic efficiencies recommended by GYTL for N, O, and NO as third bodies are 10 times greater than those of Dunn and Kang. This tenfold increase significantly enhances N recombination via reactions 5, 9, 13 in Table 1. When these third-body efficiencies are increased by 10 in Dunn and Kang's model, all computed concentrations are within 30% of those obtained with GYTL. The degree of nonequilibrium for electron populations is smaller with GYTL than with Dunn and Kang (Fig. 1), but the mechanism leading to ionizational nonequilibrium is identical. The excess free-electron population is a result of finite N atom recombination rates, and Eqs. (2–5) apply.

Mechanism of Park

Between 4000 and 10,000 K, the rate coefficients proposed by Park[4,5] are up to 140 times greater than those of Dunn and Kang,[2] except for reactions 2, 7, 8, 15, 20, 23, and 27, in which case they are smaller by up to a factor 30. In particular, the rate coefficient of the dominant electron recombination reaction 12 is about one order of magnitude greater than in Dunn and Kang's model. Nevertheless, the mechanism governing ionizational nonequilibrium is the same as with the previous models, and Eqs. (2–5) apply again (with the exception of that for O^+).

Influence of Ionizational Nonequilibrium on Plasma Radiation

The effects of ionizational nonequilibrium and discrepancies between kinetics models on the radiative emission of recombining plasmas may be illustrated for the case of NO, which is a major radiator in air plasmas.[10] For the sake of simplification, we assume that the populations n_j and n_e of bound and free electrons, respectively, are strongly coupled by collisional processes. By the excited-state Saha equation,[9] the overpopulation factor of an electronic state j is then given by

$$n_j/n_j^* = \left(n_e/n_e^*\right)^2 \tag{6}$$

With n_j^B defined as the population of level j in Boltzmann equilibrium with the ground state of NO, Eq. (6) becomes

$$n_j/n_j^B = \left(n_j^*/n_j^B\right)\left(n_e/n_e^*\right)^2 \tag{7}$$

In Eq. (7), the multiplier (n_j^*/n_j^B) is the reciprocal of the chemical nonequilibrium factor x/x^* from Fig. 1, in this case for NO. It follows from Fig. 1 that (n_j/n_j^B) varies from 1.2 with Park's mechanism to 2.2 with GYTL and 90 with Dunn and Kang. Since the radiation is proportional to excited level populations, the actual NO radiation would be from 1.2 to 90 times greater than if the excited electronic levels of NO were assumed to be in Boltzmann equilibrium with the ground state. Thus, although the electron overpopulation predictions of the three models differ only by a factor of 3, the radiative power predictions differ by up to two orders of magnitude.

Discussion

The extent of ionizational and chemical nonequilibrium under the conditions of the present study is controlled by the recombination of neutrals via the two reactions $N + O + M \rightarrow NO + M$ and $2N + M \rightarrow N_2 + M$. The modeling of plasma kinetics is greatly simplified in this case, as only two reactions must be considered vs over 30 reactions with a complete mechanism. Yet the rates recommended by Dunn and Kang,[2] GYTL,[3] and Park[5] for these two reactions differ from each other by up to one order of magnitude. We have therefore undertaken an experimental study of ionizational nonequilibrium in air and nitrogen plasmas[11] to assess the rates proposed in the three mechanisms and to test and refine the ideas presented here.

Conclusions

The present numerical study of air plasma kinetics yields the unexpected result that, as electron recombination occurs primarily via fast two-body dissociative recombination, ionizational nonequilibrium is caused under certain circumstances by slow neutral recombination. This is unlike the case for atomic plasmas wherein ionizational nonequilibrium is caused by finite three-body electron recombination rates. Although this result was illustrated here for the special case of a thermal air plasma recombining from 7500 to 4500 K in 0.6 ms, its applicability also extends to nonthermal plasmas, as mentioned earlier, and to other molecular plasmas because dissociative recombination reactions are in general much faster than three-body electron recombination reactions. Similar conclusions can also be drawn for ionizing plasmas wherein ionization is ultimately limited by molecular dissociation.

Acknowledgments

This work was supported by the U.S. Air Force Office of Scientific Research by means of Grant AF-F49620-94, under the cognizance of Robert Barker.

References

[1]Kee, R. J., Rupley, F. M., and Miller, J. A., "Chemkin-II: a Fortran Chemical Kinetics Package for the Analysis of Gas-Phase Chemical Kinetics," Sandia National Labs., SAND89-8009, Livermore, CA, Sept. 1989.

[2]Dunn, M. G., and Kang, S.-W., "Theoretical and Experimental Studies of Reentry Plasmas," NASA CR-2232, April 1973.

[3]Gupta, R. N., Yos, J. M., Thompson, R. A., and Lee, K.-P., "A Review of Reaction Rates and Thermodynamic and Transport Properties for an 11-Species Air Model for Chemical and Thermal Nonequilibrium Calculations to 30,000 K," NASA RP-1232, Aug. 1990.

[4]Park, C., *Nonequilibrium Hypersonic Aerothermodynamics*, Wiley, New York, 1990.

[5]Park, C., "Review of Chemical-Kinetic Problems of Future NASA Missions, I: Earth Entries," *Journal of Thermophysics and Heat Transfer*, Vol. 7, No. 3, 1993, pp. 385–398.

[6]Liu, Y., and Vinokur, M., "Equilibrium Gas Flow Computations. I. Accurate and Efficient Calculation of Equilibrium Gas Properties," AIAA Paper 89-1736, June 1989.

[7]Mitchner, M., and Kruger, C. H., *Partially Ionized Gases*, Wiley, New York, 1973.

[8]Sutton, G. V., and Sherman, A., *Engineering Magnetohydrodynamics*, McGraw–Hill, New York, 1965, p. 148.

[9]Kruger, C. H., Owano, T. G., Gordon, M. H., and Laux, C. O, "Nonequilibrium Effects in Thermal Plasmas," *Pure and Applied Chemistry*, Vol. 64, No. 5, 1992, pp. 607–613.

[10]Laux, C. O., Gessman, R. J., and Kruger, C. H., "Modeling the UV and VUV Radiative Emission of High-Temperature Air," AIAA Paper 93-2802, July 1993.

[11]Laux, C. O., Gessman, R. J., and Kruger, C. H., "Mechanisms of Ionizational Nonequilibrium in Air and Nitrogen Plasmas," AIAA Paper 95-1989, June 1995.